IEEE Access
Multidisciplinary | Rapid Review | Open Access Journal

Received 18 October 2022, accepted 19 November 2022, date of publication 24 November 2022, date of current version 30 November 2022.

Digital Object Identifier 10.1109/ACCESS.2022.3224473

RESEARCH ARTICLE

Single-Longitudinal-Mode Thulium-Doped Fiber Laser With Sub-kHz Linewidth Based on a Triple-Coupler Double-Ring Cavity

TING LI[1], FENGPING YAN[1], XUEMEI DU[2], WEI WANG[1], DANDAN YANG[1], XIANGDONG WANG[1], CHENHAO YU[1], KAZUO KUMAMOTO[3], (Member, IEEE), HONG ZHOU[3], AND TING FENG[4], (Member, IEEE)

[1]School of Electronic and Information Engineering, Beijing Jiaotong University, Beijing 100044, China
[2]Science and Technology on Electromagnetic Scattering Laboratory, Beijing 100089, China
[3]Department of Electronics, Information and Communication Engineering, Osaka Institute of Technology, Osaka 535-8585, Japan
[4]Photonics Information Innovation Center, Hebei Provincial Center for Optical Sensing Innovations, College of Physics Science and Technology, Hebei University, Baoding 071002, China

Corresponding author: Fengping Yan (fpyan@bjtu.edu.cn)

This work was supported in part by the National Natural Science Foundation of China under Grant 61827818, in part by the Hebei Provincial Natural Science Foundation for Outstanding Young Scholars under Grant F2020201001, and in part by the Science and Technology Research Project of Higher Education in Hebei Province under Grant QN2021050.

ABSTRACT We propose and demonstrate a stable single-longitudinal mode (SLM) thulium-doped fiber laser (TDFL) with a Fabry- Pérot (F-P) fiber Bragg grating (FBG) filter and a triple-coupler based double-ring cavity (TC-DRC) filter. For the first time, this structure of TC-DRC filter is used to select a single mode from dense longitudinal-modes in a ring cavity TDFL. The design and fabricate methods of TC-DRC filter are revealed and the principle of SLM selection is also analyzed in detail. The experimental results demonstrated the good performance of the proposed filter. The central wavelength of proposed TDFL is 2049.49 nm and its OSNR is higher than 35 dB. There is no obvious wavelength drift during the test, and the power fluctuation is less 0.5 dB. The SLM operation is verified through the self-homodyne method, this laser can be stably maintained in a SLM state after operating for one hour under laboratory condition. In addition, the linewidth is measured less than 10 kHz based on the phase noise demodulation method.

INDEX TERMS Narrow linewidth, single-longitudinal-mode, thulium-doped fiber laser.

I. INTRODUCTION

As one of the effective schemes to broaden the communication channel, 2 μm band optical technologies have become a research hotspot in recent years [1], [2], [3], [4]. Single-longitudinal-mode (SLM) Thulium-doped ring cavity fiber laser has the advantages of high output power and no spatial hole burning compared with common distributed feedback (DFB) laser and distributed Bragg reflector (DBR) laser [5], [6]. Based on its excellent SLM oscillation and narrow linewidth characteristics [7], [8], [9], SLM Thulium-doped fiber lasers are preferred light source for many applications, such as optical measurement [10], coherent light communication [11] and optical fiber sensing [12]. Due to the ultra-high spatial resolution application requirement in those areas, multiform narrowband filters are created and adopted to optimize longitudinal-mode interval [13]. [14] proposed a single cylindrical micro-resonator which has a nanoscale variation in radius to generate a peak-like transmission spectrum based on the Fano resonance effect, the peak linewidth is sufficiently small to select only one SLM oscillation in a fiber cavity. Reference [15] reported a SLM-EDF ring laser incorporating asymmetric structure filter with two PMFBG Fabry-Perot cavities. Three PM-FBGs filter can form asymmetric two cavities with different cavity lengths and effectively decrease the transmission passband bandwidth of the

The associate editor coordinating the review of this manuscript and approving it for publication was Zeev Zalevsky.

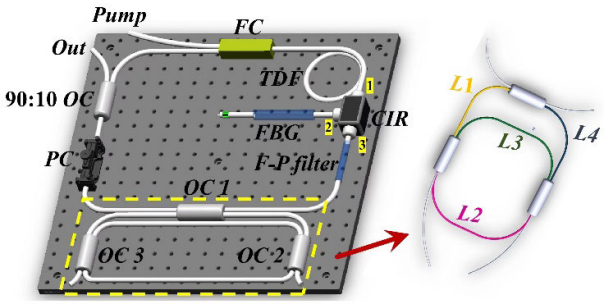

FIGURE 1. Configuration of the proposed SLM TDFL. The yellow dashed box selects the TC-DRC filter. In the illustration, $L_1 = 0.5$ m, $L_2 = 0.5$ m, $L_3 = 0.94$ m and $L_4 = 0.5$ m.

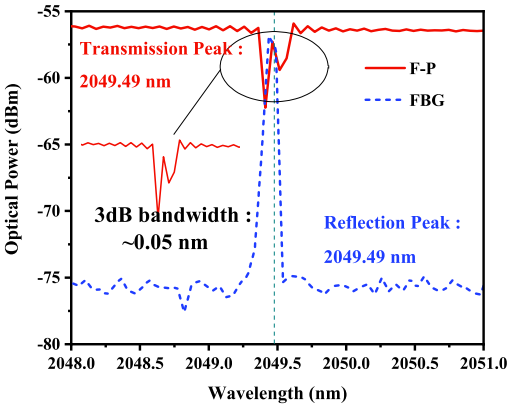

FIGURE 2. The transmission spectrum of F-P and reflection spectrum of FBG. The inset is an enlarged image of the transmission spectrum of F-P filter.

asymmetric structure filter. However, the longer cavity length also puts forward strict requirements on the ability of longitudinal mode selection, multiple optical fiber couplers cascaded to form a polycyclic subring-cavity has been utilized to realize laser SLM outputs.

In this paper, we propose and experimentally demonstrate a SLM Thulium-doped fiber laser via a novel triple-coupler based double-ring cavity (TC-DRC) filter and an F-P filter. First, we describe the proposed laser's experimental configuration, give the detailed numerical analysis of the proposed TC-DRC filter and the principle for realizing the SLM operation of the proposed laser. Next, we provide the measured characteristics of output wavelength, including the optical spectra, wavelength drift, and power fluctuation, as well as the frequency spectra for confirming SLM operation. Finally, the laser linewidth of output wavelength was measured by the in-house constructed linewidth measurement system based on the laser phase noise demodulation method. Benefiting from the neat design, this laser shows high output performances of linewidth, stability and efficiency.

II. EXPERIMENTAL SETUP AND PRINCIPLES

A. LASER CONFIGURATION

The schematic diagram of the proposed thulium-doped fiber laser system is shown in Fig. 1. A typical ring cavity structure is utilized, which mainly includes an amplified spontaneous emission source, a fiber grating combination, and a TC-DRC filter. A 4 m long thulium-doped fiber (TDF, SM-TDF-10P/130-HE, Nufern) as the gain medium is pumped by a 793 nm laser diode (LD, DS3-51512-K793DA3RN-12.00W, BWT) through a 793/2050 nm fiber pump combiner (FC). All devices utilized in this experiment are placed on the ultra-stable optical platform to avoid the disturbances of external vibration. A uniform fiber Bragg grating (UFBG) and an F-P filter are combined as a single-channel reflection filter of original wavelength selection by cooperating with a three-port optical circulator (CIR) which is also used to ensure unidirectional oscillation in the main ring cavity (MRC). In order to avoid the influence of reflected light from fiber end-face, the free end of the FBG is spliced to an FC/APC connector. A fiber squeezer polarization controller (PC) is incorporated to adjust the laser gain and loss inside the cavity. The generated laser is extracted from the 10% port of a 90:10 optical coupler (OC). The TC-DRC filter is composed by three OCs, OC1, OC2 and OC3, with coupling ratios of 90:10, 50:50 and 50:50 respectively. Three OCs with different optical ratios nest one another and form two rings as marked as ring-1 ($L1$+$L2$+$L4$) and ring-2 ($L2$+$L3$), respectively, with the lengths of 1.5 m and 1.44 m. The OC1 keep 80% energy reserved inside the TC-DRC. After our pre-testing, the insertion loss of each coupler is approximately 0.2 dB. The length of laser cavity is about 12.46 m corresponding to a longitudinal-mode spacing of 16.4 MHz.

B. PRINCIPLE OF SINGLE-WAVELENGTH OPERATIONS

The UFBG and F-P filter were fabricated by using the phase mask method in a section of hydrogen-loaded homemade single mode fiber. For the F-P filter, the lengths of two sub-gratings are all ~10mm, and the distance between two sub-gratings is ~7nm. Using an amplified spontaneous emission source, the reflection spectra of UFBG and the transmission spectra of F-P filter were measured by a Thorlabs 203C optical spectrum analyzer (OSA) as shown in the Fig. 2. The central wavelength of the UFBG reflection peak is 2049.49 nm and the reflectivity is greater than 90% (depth: >10 dB). The transmission peak of F-P FBG is 2049.49 nm and the 3 dB bandwidth is ~0.05 nm, equivalent to 3.57 GHz, as shown in Fig. 2. The reflection peak of UFBG is in good agreement with the transmission peak of F-P FBG. According to the laser structure diagram, the UFBG is connected to the port 2 of CIR as a reflection mirror and the F-P FBG is located in port 3. Therefore, this group of gratings can be used as a gross filter in the laser cavity, the output wavelength of designed TDFL can be determined in 2049.49 nm.

C. PRINCIPLES OF SLM LASING

Fig. 3 shows the running schematic of the proposed TC-DRC filter formed by OC1, OC2 and OC3. We set L_1–L_4 as the lengths of fibers as marked, E_1–E_{15} as the electric field amplitudes of ports of OCs, α_i ($i = 1, 2, 3$) and γ_j ($j = 1, 2, 3$) respectively as the coupling ratio and insertion loss of the OCs, β as the fiber loss coefficient, δ as the fusion

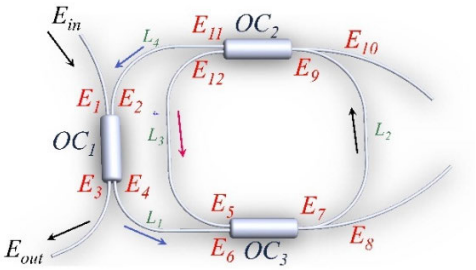

FIGURE 3. The components of the TC-DRC filter. E_{in}, $E_2 \ldots E_{12}$, E_{out} are field intensities of different OC ports, the arrows indicate the laser transmission direction in the loops.

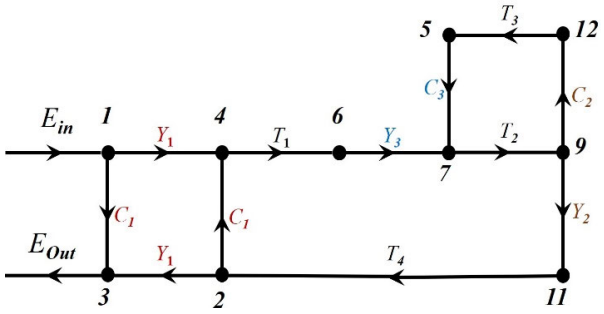

FIGURE 4. Signal-flow graph representation of the sub-ring cavity.

splicing loss, $k = 2\pi/\lambda$ as the wave number and n_{eff} as the effective refractive index of the SMF.

A graphical method called signal-flow graph is introduced in this research to understand the compound ring sub-cavity system operation using a pictorial representation. The signal-flow graph was originally proposed by S. J. Mason [16], to obtain the causal relationship of the signal transformation and transmission in electrical circuits [17]. This method can directly obtain the transfer function without taking complicated mathematical operation. According to the Fig. 3, the signal-flow graph of sub-ring cavity is shown in Fig. 4. In order to analyze the transitive relation from node E_{in} to E_{out} using Mason's rule, we need to analyze the dependence of 10 nodes among each other and the path and loop gains of signal-flows firstly, based on the signal-flow graph in Fig. 4. The straight transmittances of OCs are defined as C_i

$$C_i = \sqrt{1-\gamma_i}\sqrt{1-k_i} \quad (i = 1, 2, 3) \tag{1}$$

The cross-coupling transmittance Y_i of three OCs as

$$Y_i = j\sqrt{k_i}\sqrt{1-\gamma_i} \quad (i = 1, 2, 3) \tag{2}$$

And the propagating gain T_i of fiber optical paths L_i as

$$T_i = \sqrt{1-\delta}\exp\left(-\alpha + j\beta\right) L_i \quad (i = 1, 2, 3, 4) \tag{3}$$

There are double loops in Fig. 3, respectively involving the optical nodes 4-6-7-9-11-2-4 and 7-9-12-5. According to the Eq. (1) to (3), the inflow and outflow relationship of optical signals between each node can be expressed as follow:

$$\begin{aligned}
E_1 &= E_{in} = 1 \\
E_3 &= C_1E_1 + Y_1E_2 = E_{Out}E_4 = C_1E_2 + Y_1E_1 \\
E_6 &= T_1E_4 \\
E_7 &= C_2E_5 + Y_2E_6 \\
E_9 &= T_2E_7 \\
E_{11} &= C_3E_{10} + Y_3E_9E_{12} = C_3E_9 + Y_3E_{10} \\
E_5 &= T_3E_{12} \\
E_2 &= T_4E_{11}
\end{aligned} \tag{4}$$

As shown in Fig. 3, when the incident light passes through the TC-DRC filter for the first time, the incident light intensity of port 2 of OC1, port 5 of OC3 and port 10 of OC2 are all 0 ($E_2 = 0$, $E_5 = 0$ and $E_{10} = 0$). The Eq. (4) can be broken down into a matrix form for easy solution, (5), as shown at the bottom of the next page.

According to the Eq. (5), the electric field amplitudes of OCs can be obtained readily:

$$E = M^{-1}B \tag{6}$$

Therefore, based on Eqs. (1)-(6), the transmission T of TC-DRC filter can be obtained as

$$T = \frac{I_{Output}}{I_{Input}} = \left(\frac{E_3}{E_1}\right) \cdot \left(\frac{E_3}{E_1}\right)^* \tag{7}$$

Based on the theory above, the transmission spectrum of TC-DRC filter can be simulated by MATLAB. According to the measurement of fiber Bragg grating spectrum, the 3 dB bandwidth of F-P filter is 0.05 nm, corresponding to a frequency range of ~18 GHz. In this ring cavity TDFL, this double-ring compound sub-cavity is utilized as an ultra-narrow comb filter to select SLM. The free space range (FSR) of ultra-narrow comb filter must be larger than 0.5 times and less than 1 times of F-P filter's transmission bandwidth. For the same reason, the passband of ultra-narrow comb filter must be 1 to 2 times of MRC's mode-spacing. There is only SLM selected from dense modes in the grating bandwidth through this method. In the process of designing the parameters of TC-DRC, the fiber loss coefficient β, the fusion splicing loss δ, the effective refractive index of the SMF n_{eff} and the insertion loss of OCs are setting as constants. The length of sub-cavity L_i and the coupling ratio of OCs α_i are varied to optimize the transmission performance of TC-DRC filter. The α_i mainly affects the Q value of the laser cavity, that is, the storage capacity of the laser cavity for energy, and the cavity length L_i determines the FSR of TC-DRC filter. The calculation formula of FSR is shown as follow:

$$FSR = \frac{c}{n_{eff}L_{cavity}} \tag{8}$$

where c is the speed of light in vacuo. It can be seen the FSR of sub-cavity is inversely proportional to L_{cavity} from Eq. (8).

Fig. 5 and Fig. 6 show the simulation results of different α_i and L_i. In the designed sub-cavity, the lengths of ring-1 and ring-2 are composed by $L_1 + L_2 + L_4$ and $L_2 + L_3$, respectively. Here, we introduce the optical vernier effect [18], [19], a small cavity length difference is introduced between the double rings, the effective FSR of the sub-cavity can be greatly extended. As seen in Fig. 5(a), 5(b) and 5(c),

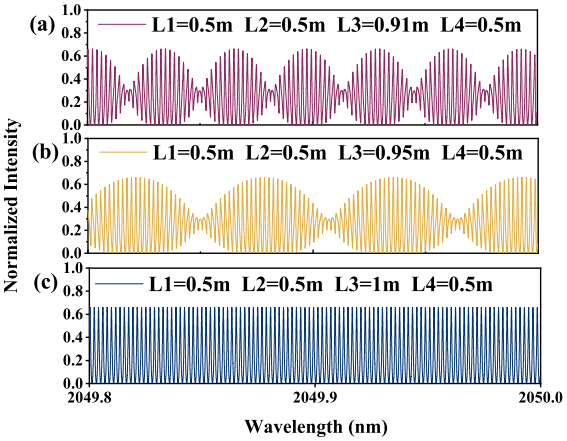

FIGURE 5. The simulation results of proposed sub-ring cavity. (a), (b) and (c) are the influence of sub-ring cavity length on transmission performance.

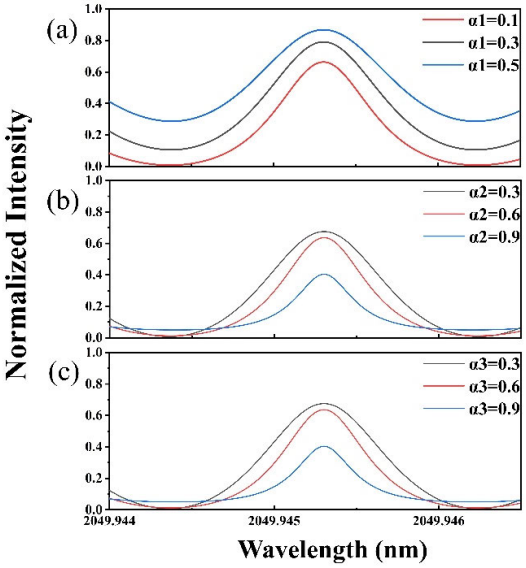

FIGURE 6. The simulation results of proposed sub-ring cavity. (a), (b) and (c) are the influence of coupler ratio on sub-ring cavity transmission, $\alpha 2$ and $\alpha 3$ have the same effect because they are in a symmetric structure.

the ring length differences between double ring are 0.09 m, 0.05 m and 0m, respectively. With the decrease of ring length difference, the FSR of transmission spectrum increase gradually. In the design process of sub-cavity, the 3 dB bandwidth of F-P filter is 0.05 nm, which means the FSR of sub-cavity must be between 1.78 GHz and 3.56 GHz.

When the coupling ratio of OC1 and OC2 are fixed values, the bandwidth of sub-cavity transmission peak changes with α_1 is shown in Fig. 6 (a). The bandwidth of transmission peak is proportional to the OC1's coupling ratio and the transmittance increases with α_1. According to the Fig. 2, OC2 and OC3 are inserted in a symmetric position to construct sub-cavity, their coupling ratios have the same effect on the transmission performance. Fig. 6 (b) shows the relationship between transmission peak bandwidth and α_2. The bandwidth of transmission peak decreases significantly with the increase of α_2, this characteristic is helpful for designing reasonable ultra-narrow filter. The transmissivity, meanwhile, become lower and lower with the increase of α_2. Therefore, the length of sub-cavity and the coupling ratio of OCs must be designed

$$M = \begin{bmatrix} 1 & 0 & 0 & 0 & 0 & 0 & 0 & 0 & 0 & 0 & 0 & 0 \\ 0 & -1 & 0 & 0 & 0 & 0 & 0 & 0 & 0 & 0 & T_4 & 0 \\ C_1 & Y_1 & -1 & 0 & 0 & 0 & 0 & 0 & 0 & 0 & 0 & 0 \\ Y_1 & C_1 & 0 & -1 & 0 & 0 & 0 & 0 & 0 & 0 & 0 & 0 \\ 0 & 0 & 0 & 0 & -1 & 0 & 0 & 0 & 0 & 0 & 0 & T_3 \\ 0 & 0 & 0 & T_1 & 0 & -1 & 0 & 0 & 0 & 0 & 0 & 0 \\ 0 & 0 & 0 & 0 & C_3 & Y_3 & -1 & 0 & 0 & 0 & 0 & 0 \\ 0 & 0 & 0 & 0 & Y_3 & C_3 & 0 & -1 & 0 & 0 & 0 & 0 \\ 0 & 0 & 0 & 0 & 0 & 0 & T_2 & 0 & -1 & 0 & 0 & 0 \\ 0 & 0 & 0 & 0 & 0 & 0 & 0 & 0 & 0 & -1 & 0 & 0 \\ 0 & 0 & 0 & 0 & 0 & 0 & 0 & 0 & Y_2 & C_2 & -1 & 0 \\ 0 & 0 & 0 & 0 & 0 & 0 & 0 & 0 & C_2 & Y_2 & 0 & -1 \end{bmatrix},$$

$$E = \begin{bmatrix} E_1 \\ E_2 \\ E_3 \\ E_4 \\ E_5 \\ E_6 \\ E_7 \\ E_8 \\ E_9 \\ E_{10} \\ E_{11} \\ E_{12} \end{bmatrix}, \quad B = \begin{bmatrix} 1 \\ 0 \\ 0 \\ 0 \\ 0 \\ 0 \\ 0 \\ 0 \\ 0 \\ 0 \\ 0 \\ 0 \end{bmatrix}, \; ME = B \tag{5}$$

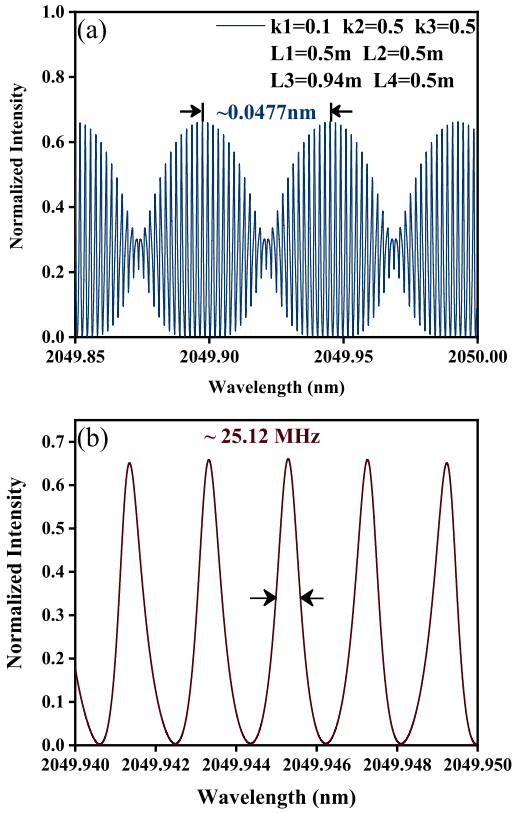

FIGURE 7. The optimized transmission spectrum of sub-cavity. (a). The FSR of sub-cavity is ∼0.0477nm, equivalent to 3.41 GHz. (b). The FWHM of transmission peak is ∼25.12 MHz.

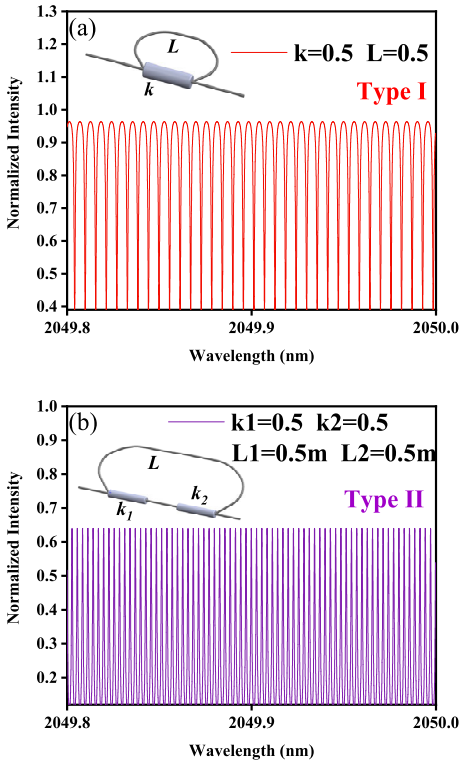

FIGURE 8. The transmission spectrum of fiber ring. L_i is the length of coupler fiber arms and k_i is the coupling ratio of OCs.

properly. After many optimizations, the final parameters of sub-cavity are shown in Fig. 7. The FSR of TC-DRC filter envelope is ∼0.0477 nm, corresponding frequency is about 3.41 GHz. The transmission peak bandwidth of the TC-DRC filter is measured as ∼25.12 MHz. As mentioned above, the proposed TC-DRC filter has excellent SLM selection ability in 12.46 m cavity length TDFL.

In the development of ring cavity SLM fiber laser, two types basic fiber ring structures are usually used as secondary cavities for SLM fiber laser. One is composed with a single OC (Type I) [20]; the other is based on two OCs with identical coupling ratios (Type II) [21]. The transmission spectrums of above two classical fiber rings are shown in Fig. 8. The insets show the classic structure of two types fiber ring, where k_i is the coupling ratio of OCs and L_i is the length of fiber ring. The FSR and FWHM of fiber rings are also subject to k_i and L_i, both types of basic fiber rings have only one sub-ring cavity. According to the Eq. (8), the sub-ring cavity needs a long cavity length to obtain suitable FSR which can match the 3dB bandwidth of FBG. Meanwhile, the cavity length of the whole ring cavity laser will increase greatly, and the longitudinal mode interval of the main cavity will also become narrower. This means that more difficult to handle sub-cavity parameters to achieve SLM selection. In conclusion, the TC-DRC filter proposed in Fig. 2 has excellent capacity to select SLM in ring cavity fiber laser.

III. EXPERIMENTAL RESULTS AND DISCUSSION

We carried out all experiments at laboratory temperature and did not employ any extra vibration isolation and temperature compensation techniques for the TDFL system which was just built and constructed on an ordinary aluminum optical breadboard. The lasing threshold of the TDFL was measured to be 2.77 W. Initially, the spectrum of single-wavelength operation is recorded by OSA, as shown in Fig. 9. The center wavelength of the output laser is 2049.49nm, which is in good agreement with the transmission peak wavelength of F-P FBG, the OSNR of single-wavelength is 35.58 dB. For the demonstration stability of single-wavelength operation, we took 10 repeated OSA scans at ∼6 min intervals in a time span of over 1 hours (∼60 min) during nighttime, as shown in the inset of Fig. 9 (a), the three-dimensional (3-D) plot, which shows little or no variations of either the wavelength or the power. Furthermore, as can be seen in Fig. 9 (b) and (c) plotted using the data extracted from the 3-D figure, the measured wavelength drift is less than 0.004nm, which is less than the OSA's resolution and also indicating the central wavelength is extremely stable; the corresponding power-fluctuations is less than 0.5 dB. These data indicates that proposed TDFL has an outstanding performance of stability, which mainly benefits from the excellent mode-selection capability of the TC-DRC filter.

The SLM operation of laser output was verified by using the self-homodyne method when the pump power was fixed at 2.9 W. The measurement setup included a 1 GHz photodetector (CONQUER KG-PR-1G-20) with a strong response in

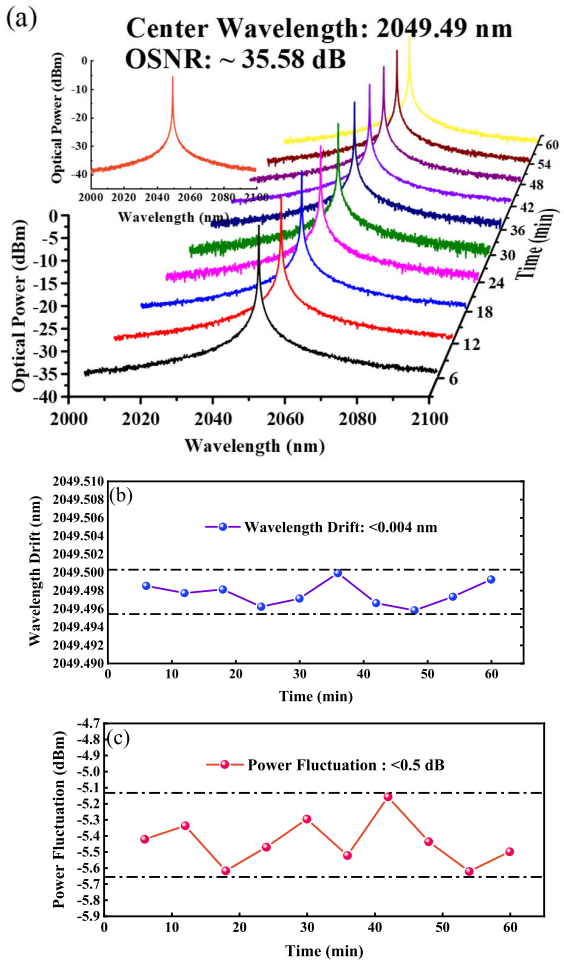

FIGURE 9. Spectra of single-wavelength operation lasing at 2049.4985 nm. (a) 10 repeated spectra measured by OSA with a time interval of ~6 min. (b) Wavelength drift of single wavelength during 60 mins. (c) Power fluctuation of single wavelength during 60 mins.

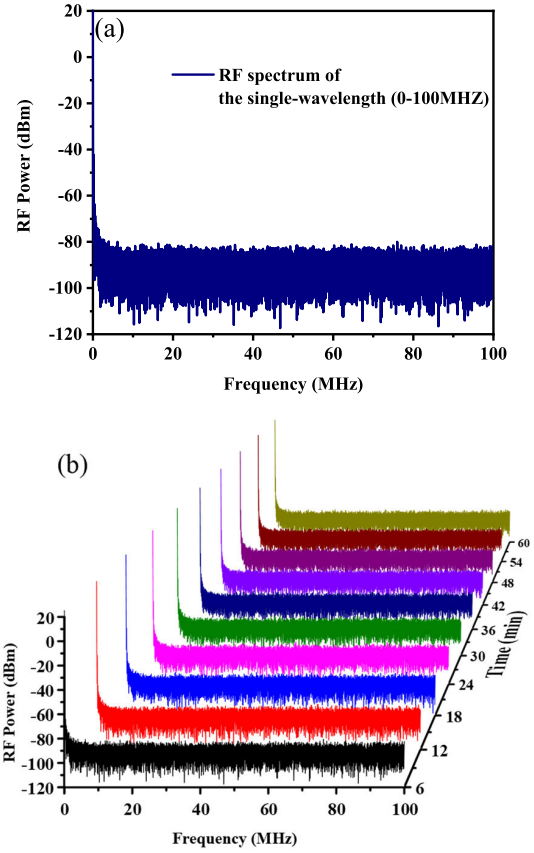

FIGURE 10. (a) The self-homodyne RF spectrum measured by FSA for single wavelength of 2049.4985 nm with a range of 0-100 MHz. (b) The RF spectrum measured every 10 mins.

the 2 μm band and an 8 GHz radio-frequency (RF) electrical spectrum analyzer (ESA, R&SFSH8 handheld spectrum analyzer). The scanning range of ESA was setting to 0-100 MHz and the resolution was 10 kHz, as shown in Fig. 10 (a), the scanning range is much wider than the spacing between two adjacent longitudinal modes. No conspicuous beat RF signal can be observed below 100 MHz, which indicates that the proposed TDFL operates in SLM stably. Still, Fig. 10 (b) is the RF beating spectra measured every 60 mins within one hour. We can see that there was no beating signal captured for lasing wavelength, and the laser operated in a stable SLM state.

To verify the longitudinal mode selection capability of the TC-DRC, the RF beating spectra of the laser without the sub-cavity spliced inside the cavity were measured for single-wavelength operation and shown in Fig. 11 (c). The numerous spikes in the spectra indicate lasing in multi-longitudinal modes. The spacing of adjacent peaks is about 16.4 MHz, corresponding to a laser cavity length of 12.46 m for the MRC.

To further investigate the linewidth characteristics of the proposed TDFL, an imbalanced Michelson interferometer (MI) composed of a 3 $\times$ 3 coupler and two Faraday rotation mirrors (FRMs) was set for laser phase noise demodulation [22], [23], 24], as shown in Fig. 12 (a). A 50-m length standard single-mode fiber (SMF) was incorporated in an interferometer instead of the overlong delay line that has to be used in the traditional delayed self-heterodyne linewidth measurement method, as the transmission loss of 2 μm light is high. The incident lasing launched into port 1 was spliced through the 3 $\times$ 3 coupler into arm 4, arm 5, and an unused arm 6. A 50-m-long SMF was inserted into arm 5 as the delay line, which introduced a time delay τ between the two arms. After being reflecting by the two FRMs, the light in the arms returned to the coupler, underwent interference, and was then fed into PD1 and PD2 through arm 2 and arm 3. The received interference fringes, containing information about the differential phase fluctuation accumulated in the delay time τ of the MI, were uploaded by the OSC to a computer to calculate the power spectral density (PSD) of the laser's instantaneous phase fluctuation $S_\varphi(f)$ and frequency fluctuation $S_V(f)$ [23]. The laser linewidth could then be calculated using the β separation line method ($\beta = S_V(f) = (8\ln 2/\pi^2)\cdot f$) [25]. By calculating the geometrical area under the frequency noise PSD obtained for all Fourier frequencies exceeding the β separation line, the FWHM laser linewidth at different integration bandwidths was approximated using

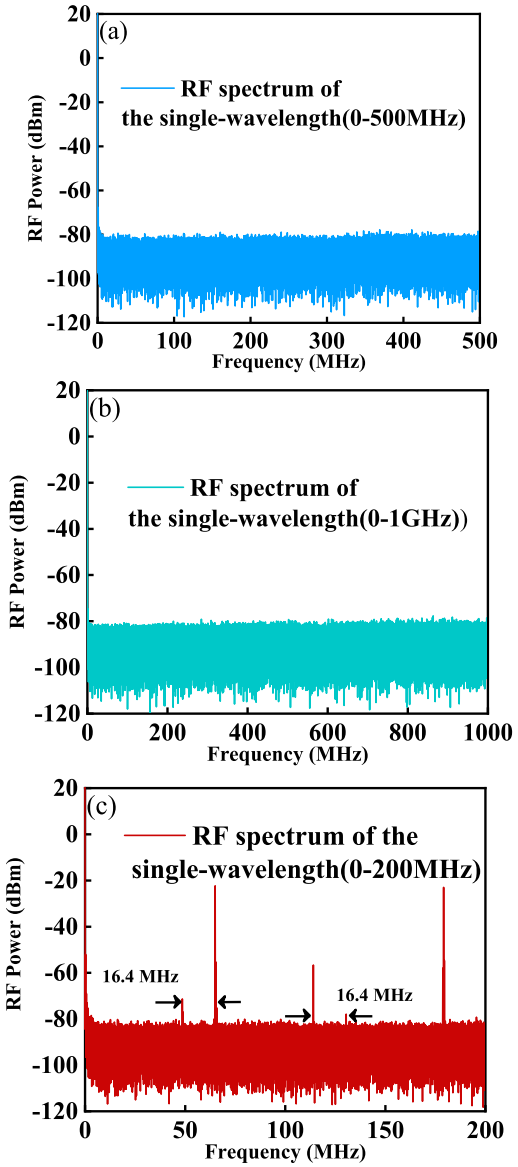

FIGURE 11. The RF beating spectra of laser output (a) with TC-DRC filter in 0-500 MHz. (b) with TC-DRC filter in 0-1 GHz. (c) without TC-DRC filter.

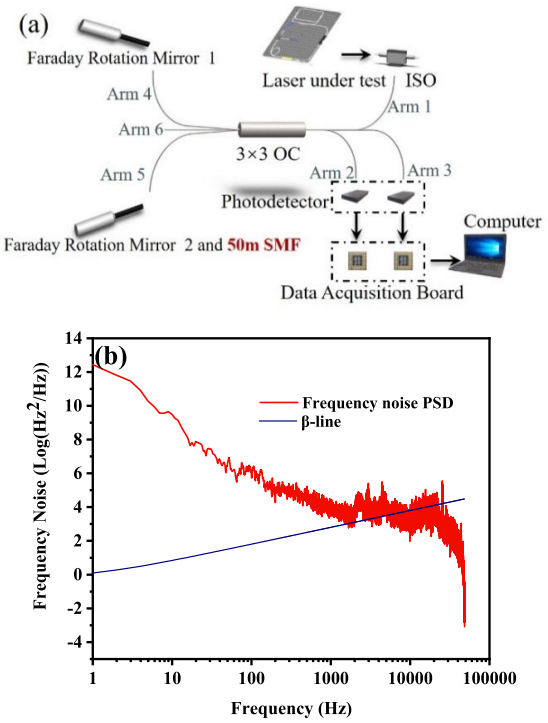

FIGURE 12. (a) Configuration of the linewidth measurement system. (b) The frequency noise power spectral density of an SLM laser at 2049.49nm.

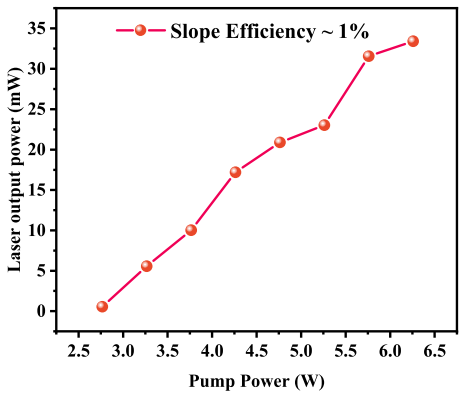

FIGURE 13. Laser output power varies with the input pump power.

the relation: $FWHM = \sqrt{8 \ln 2A}$ [24]. Fig. 12 (b) shows the measured frequency noise PSD for 2049.49 nm wavelength, which is measured in the mode of maximum sampling time of 1s. Meanwhile, the linewidths on different time scales 0.001 s, 0.005 s, 0.01 s, 0.05 s, 0.1 s, 0.5 s, and 1 s of incident laser are also measured, corresponding numerical values are 5.04, 14.63, 22.17, 61.05, 167.81, 643.64 and 2758.09 kHz, respectively. When the measurement time is the minimum 0.001 s, the linewidth of incident 2049.49 nm laser is less than 10kHz. When the measurement time is the maximum 1 s, the linewidth of incident 2049.49 nm laser is more than 2500kHz, which is caused by physical vibration and low-frequency signal interference during the measurement process. In addition, the thermal noise generated by the continuous pumping of laser cladding pump also affects the measurement results. To sum up, the linewidth of proposed TDFL is $<$10kHz.

As an important index to estimate the output power performance, the slop efficiency of proposed TDFL with a wavelength of 2049.49 nm acquired by a power meter (Laser point) is shown in Fig. 13. The slope efficiency of fiber laser can be calculated as:

$$e_{slope} = \frac{P_{Out}}{P_{in} - P_{threshold}} \tag{9}$$

The threshold of proposed TDFL is 2.77 W, corresponding output power is 0.43 mW. The low slope efficiency of $\sim$1% is mainly due to the low transmission of TC-DRC for SLM selection and the field mismatch loss during the fusion splicing between the octagonal cross-section TDF and the circulator common SMF pigtail. As can be seen from the Fig. 13, the curve is not saturated. In order to avoid the irreversible influence of the thermal effect caused by excessive laser

pumping on the intracavity devices, the pump injection power was not increased.

IV. CONCLUSION

In summary, an ultra-narrow linewidth single-longitudinal-mode thulium-doped fiber laser was analyzed and experimentally demonstrated. In this laser, a uniform FBG and a narrow band F-P filter were incorporated in the cavity to act as the wavelength selector. The 3dB bandwidth of F-P filter transmission peak was approximate 0.05nm. A novel passive dual ring compound sub-cavity made with three different OCs was utilized for SLM selection, and the SLM selection ability of this TC-DRC filter was theoretically analyzed and experimentally verified. The good laser output performances were also presented in detail. We believe this is the first time that this kind of specially-designed TC-DRC has been used in a 2 μm fiber laser for SLM operation. For the obtained laser output, the maximum OSNR was 35.58 dB, the maximum wavelength fluctuation was 0.004 nm, and the maximum power fluctuation was 0.5 dB. During the hour-long monitoring session, the output laser was always in a stable SLM state. In addition, the measured laser linewidth was less than 10 kHz, which was comparable to the reported SLM lasers in this wavelength range. In a follow-up study, on the basis of TC-DRC filter, switchable SLM TDFL can be easily realized by replacing with multichannel FBG. We believe that our proposed laser has great potential for application in coherent optical communication and optical measurement systems.

REFERENCES

[1] S. Jeffress, "Silicon photonic flat-top WDM (de)multiplexer based on cascaded Mach–Zehnder interferometers for the 2 μm wavelength band: Publisher's note," *Opt. Exp.*, vol. 30, p. 15, Aug. 2022.

[2] E. M. Scherrer, B. E. Kananen, E. M. Golden, F. K. Hopkins, K. T. Zawilski, P. G. Schunemann, L. E. Halliburton, and N. C. Giles, "Defect-related optical absorption bands in CdSiP_2 crystals," *Opt. Mater. Exp.*, vol. 7, no. 3, p. 658, 2017.

[3] X. Ma, S. Liu, W. Dai, W. Chen, L. Tong, S. Ye, Z. Zheng, Y. Wang, Y. Zhou, W. Zhang, and W. Fang, "Application of TiCN on passively harmonic mode-locked ultrashort pulse generation at 2 μm," *Opt. Laser Technol.*, vol. 150, Jun. 2022, Art. no. 107986.

[4] X. Cao, Q. Zhu, A. Xian, Y. Liu, G. Liu, L. Li, X. Li, X. Xu, W. Zhou, H. Wang, H. Huang, B. Jia, Y. Wang, J. Wang, D. Tang, and D. Shen, "Ultrafast tm:$CaYAlO_4$ laser with pulse regulation and saturation parameters evolution in the 2 μm water absorption band," *Opt. Laser Technol.*, vol. 152, Aug. 2022, Art. no. 108096.

[5] L. Zhang, "Single-frequency Tm-doped fiber laser with 215 mW at 2.05 μm based on a Tm/Ho-codoped fiber saturable absorber," *Opt. Lett.*, vol. 47, no. 15, pp. 3964–3967, 2022.

[6] L. Zhang, "Watt-level 1.7-μm single-frequency thulium-doped fiber oscillator," *Opt. Exp.*, vol. 29, no. 17, pp. 27048–27056, 2021.

[7] S. Chen, Q. Wang, C. Zhao, Y. Li, H. Zhang, and S. Wen, "Stable single-longitudinal-mode fiber ring laser using topological insulator-based saturable absorber," *J. Lightw. Technol.*, vol. 32, no. 22, pp. 4438–4444, Nov. 15, 2014.

[8] W. Li, J. Zou, Y. Huang, K. Wang, T. Du, S. Jiang, and Z. Luo, "212-kHz-linewidth, transform-limited pulses from a single-frequency Q-switched fiber laser based on a few-layer Bi_2Se_3 saturable absorber," *Photon. Res.*, vol. 6, no. 10, p. C29, 2018.

[9] T. Yin, "400 mW narrow linewidth single-frequency fiber ring cavity laser in 2 μm waveband," *Opt. Exp.*, vol. 27, no. 11, pp. 15794–15799, 2019.

[10] G. A. Cranch, P. J. Nash, and C. K. Kirkendall, "Large-scale remotely interrogated arrays of fiber-optic interferometric sensors for underwater acoustic applications," *IEEE Sensors J.*, vol. 3, no. 1, pp. 19–30, Feb. 2003.

[11] T. Feng, "Wavelength-switchable ultra-narrow linewidth fiber laser enabled by a figure-8 compound-ring-cavity filter and a polarization-managed four-channel filter," *Opt. Exp.*, vol. 29, no. 20, pp. 31179–31200, 2021.

[12] J. Cui, H. Dang, K. Feng, W. Yang, T. Geng, Y. Hu, Y. Zhang, D. Jiang, X. Chen, and J. Tan, "Stimulated Brillouin scattering evolution and suppression in an integrated stimulated thermal Rayleigh scattering-based fiber laser," *Photon. Res.*, vol. 5, no. 3, p. 233, 2017.

[13] Z. Wang, J. Shang, S. Li, K. Mu, Y. Qiao, and S. Yu, "All-polarization maintaining single-longitudinal-mode fiber laser with ultra-high OSNR, sub-KHz linewidth and extremely high stability," *Opt. Laser Technol.*, vol. 141, Sep. 2021, Art. no. 107135.

[14] H. Wang, R. Xu, J. Zhang, W. Zhou, and D. Shen, "Ultranarrow filter based on Fano resonance in a single cylindrical microresonator for single-longitudinal-mode fiber lasers," *Opt. Exp.*, vol. 27, no. 16, pp. 22717–22726, 2019.

[15] B. Yin, S. Feng, Y. Bai, Z. Liu, and S. Jian, "Switchable dual-wavelength SLM fiber laser using asymmetric PMFBG Fabry–Perot cavities," *IEEE Photon. Technol. Lett.*, vol. 27, no. 12, pp. 1281–1284, Jun. 15, 2015.

[16] S. J. Mason, "Feedback theory-some properties of signal flow graphs," *Proc. IRE*, vol. 44, no. 7, pp. 920–926, 1956.

[17] L. N. Binh, S. F. Luk, and N. Q. Ngo, "Amplified double-coupler double-ring optical resonators with negative optical gain," *Appl. Opt.*, vol. 34, no. 27, p. 6086, 1995.

[18] T. Feng, M. Wang, X. Wang, F. Yan, Y. Suo, and X. S. Yao, "Switchable 0.612-nm-spaced dual-wavelength fiber laser with sub-kHz linewidth, ultra-high OSNR, ultra-low RIN, and orthogonal polarization outputs," *J. Lightw. Technol.*, vol. 37, no. 13, pp. 3173–3182, Jul. 1, 2019.

[19] C. C. Lee, "Single-longitudinal-mode fiber laser with a passive multiple-ring cavity and its application for video transmission," *Opt. Lett.*, vol. 23, no. 5, pp. 358–360, 1998.

[20] F. Yin, S. Yang, H. Chen, M. Chen, and S. Xie, "60-nm-wide tunable single-longitudinal-mode ytterbium fiber laser with passive multiple-ring cavity," *IEEE Photon. Technol. Lett.*, vol. 23, no. 22, pp. 1658–1660, Nov. 15, 2011.

[21] J. Zhang, C.-Y. Yue, G. W. Schinn, W. R. L. Clements, and J. W. Y. Lit, "Stable single-mode compound-ring erbium-doped fiber laser," *J. Lightw. Technol.*, vol. 14, no. 1, pp. 104–109, Jan. 1996.

[22] L. Zhang, F. Yan, T. Feng, W. Han, B. Guan, Q. Qin, Y. Guo, W. Wang, Z. Bai, H. Zhou, and Y. Suo, "Six-wavelength-switchable narrow-linewidth thulium-doped fiber laser with polarization-maintaining sampled fiber Bragg grating," *Opt. Laser Technol.*, vol. 136, Apr. 2021, Art. no. 106788.

[23] D. Xu, "Laser phase and frequency noise measurement by Michelson interferometer composed of a 3×3 optical fiber coupler," *Opt. Exp.*, vol. 23, no. 17, pp. 22386–22393, 2015.

[24] Y. Bai, F. Yan, T. Feng, W. Han, L. Zhang, D. Cheng, Z. Bai, and X. Wen, "Demonstration of linewidth measurement based on phase noise analysis for a single frequency fiber laser in the 2 μm band," *Laser Phys.*, vol. 29, no. 7, Jul. 2019, Art. no. 075102.

[25] G. Di Domenico, S. Schilt, and P. Thomann, "Simple approach to the relation between laser frequency noise and laser line shape," *Appl. Opt.*, vol. 49, no. 25, pp. 4801–4807, 2010.

TING LI received the M.S. degree from the School of Optical Engineering, Minzu University, in 2019. He is currently pursuing the Ph.D. degree with the Key Laboratory of All Optical Network and Advanced Telecommunication Network, Ministry of Education, Institute of Lightwave Technology (ILT), Beijing Jiaotong University. His current research interests include rare-earth doped optical laser, single-longitudinal-mode narrow linewidth fiber laser, and multi-wavelength fiber laser.

FENGPING YAN received the B.S. degree from the Hefei University of Technology, Hefei, China, in 1989, and the Ph.D. degree from Beijing Jiaotong University, Beijing, China, in 1996. In 1996, he joined the Institute of Lightwave Technology (ILT), Beijing Jiaotong University, and was promoted as an Associate Professor, in 1998. From 2001 to 2002, he was the National Senior Visiting Scholar at the Osaka Institute of Technology, Osaka, Japan. In 2003, he was a Full Professor and became the Vice Director at the ILT, Beijing Jiaotong University. In 2018, he was the Director of the ILT, Beijing Jiaotong University. He has published more than 240 papers, written one book, and held more than 50 patents. His research interests include rare-earth-doped fibers, fiber lasers, optical wavelength switching, all optical networks, and metamaterials research. He has been chairing nine projects funded by the National Natural and Science Foundation of China, since 2000 and two projects funded by the National High Technology Research and Development Program of China (863 Program), in 1996 and 2002, respectively.

XUEMEI DU received the Ph.D. degree in electronic science and technology from Beijing Jiaotong University, in 2022. Now she is working with the Science and Technology on Electromagnetic Scattering Laboratory. Her current research interests include the research and application of metamaterial absorbers, and the integration of two-dimensional novel materials.

WEI WANG received the B.S. degree in information and computing science from the North University of China, Taiyuan, China, in 2009, and the M.E. degree form the Capital University of Economics and Business, Beijing. He is currently pursuing the Ph.D. degree in functional devices based on metamaterials with the Key Laboratory of All Optical Network and Advanced Telecommunication of Electromagnetic Compatibility, Institute of Lightwave Technology, Beijing Jiaotong University, Beijing, China.

DANDAN YANG received the master's degree in communication and information system from the Key Laboratory of All Optical Network and Advanced Telecommunication Network, Ministry of Education, Institute of Lightwave Technology (ILT), Beijing Jiaotong University, in 2019, where she is currently pursuing the Ph.D. degree with the School of Electronic and Information Engineering. Her current research interests include rare-earth doped optical laser, and single-frequency fiber laser.

XIANGDONG WANG was born in Shanxi, China, in December 1992. He received the M.S. degree from Beijing Jiaotong University, in 2019, where he is currently pursuing the Ph.D. degree with the School of Electronic and Information Engineering. His research interests include rare-earth doped optical laser, and laser communication.

CHENHAO YU received the master's degree in communication and information system from the Key Laboratory of All Optical Network and Advanced Telecommunication Network, Ministry of Education, Institute of Lightwave Technology (ILT), Beijing Jiaotong University, in 2018, where he is currently pursuing the Ph.D. degree with the School of Electronic and Information Engineering. His current research interests include rare-earth doped optical laser and optical design.

KAZUO KUMAMOTO (Member, IEEE) was born in Hiroshima, Japan, in February 1976. He received the M.S. and Ph.D. degrees from Osaka University, Japan, in 1999 and 2002, respectively. He joined the Department of Electronics, Information Systems Engineering, Osaka Institute of Technology (OIT), Japan, as a Lecturer, since 2002. He has promoted to an Associate Professor, in 2009. His research interests include FSO communications, radio over fiber systems, and mobile ad-hoc networks. He is a member of IEICE. He was awarded the Young Scientist Award of URSI from Asia Pacific Radio Science Conference, in 2010.

HONG ZHOU received the B.S. degree in electronic engineering from Tsinghua University, in 1983, and the M.S. and Ph.D. degrees in electronic engineering from Kyoto University, in 1987 and 1991, respectively. He is currently a Professor with the Department of Electronic Information and Communication Engineering, Osaka Institute of Technology. His current interests include high speed optical communication, wireless networks, and optical wireless communication.

TING FENG (Member, IEEE) received the Ph.D. degree in communication and information system from Beijing Jiaotong University, Beijing, China, in January 2015.

From September 2012 to September 2013, he was a Visiting Scholar at the Optics Laboratory, School of Electrical and Computer Engineering, Georgia Institute of Technology, Atlanta, GA, USA. He joined the Photonics Information Innovation Center, College of Physics Science and Technology, Hebei University, Baoding, China, in 2015, where he was promoted as a Full Professor, in 2021. In 2020, he was promoted as an Outstanding Young Scholar of Hebei and a Hebei new century "333 talent project" suitable person. He has authored more than 90 refereed journal articles, written two optics related books, and been granted with more than 30 patents in related areas. His research interests include optical fiber lasers, optical fiber sensing, and their application technologies. He is a member of the Optical Society of America (OSA) and Chinese Optical Society (COS). He has chaired and participated in more than ten research projects funded by the National Natural Science Foundation of China and Natural Science Foundation of Hebei.